

Supporting Information for

Remarkably high temperature spin transition exhibited by two new metal-organic frameworks

Xin Bao,^a Peng-Hu Guo,^a Wei Liu,^a Jiri Tucek,^b Wei-Xiong Zhang,^a Ji-Dong Leng,^a Xiao-Ming Chen,^a

Il'ya Gural'skiy,^c Lionel Salmon,^c Azzedine Bousseksou^c and Ming-Liang Tong*^a

^a Key Laboratory of Bioinorganic and Synthetic Chemistry of Ministry of Education, State Key Laboratory of Optoelectronic Materials and Technologies, School of Chemistry and Chemical Engineering, Sun Yat-Sen University, Guangzhou 510275, P. R. China

^b Regional Centre of Advanced Technologies and Materials, Department of Experimental Physics, Faculty of Science, Palacky University, Slechtitelu 11, 783 71 Olomouc, Czech Republic.

^c Laboratoire de Chimie de Coordination, UPR 8241 CNRS, 205 Route de Narbonne, 31077 Toulouse, France

Corresponding author: tongml@mail.sysu.edu.cn

Contents of the Supporting Information

1. Materials and General Procedures
2. PXRD Spectra
3. X-Ray Crystallography
4. Magnetic measurements
5. DSC measurements
6. Mössbauer measurements
7. Variable temperature Raman spectra measurements
8. Simulation of the two-step SCO behaviors of **1** and **2**

Fig. S1. Variable PXRD patterns for **1** (above) and **2** (below).

Fig. S2. TG curves for **1** (in black) and **2** (in red) under N₂ atmosphere.

Fig. S3. PXRD patterns of **1** as-synthesized (green) and of **1** immersing in morpholine (blue), pyridine (red) and DMF (black) for one month.

Fig. S4. Structural illustrations of **1**.

Fig. S5. Experimental PXRD (red continuous line) and Rietveld refined pattern (blue circles) and difference patterns (black line) for **2** at 600 K.

Fig. S6. The experimental $\chi_M T$ versus T curves of **1** and **2** in the temperature range 2-600 K.

Fig. S7. Mössbauer spectrum of **2** and tentative fitting results at 453 K.

Fig. S8. Scheme of spin transition route for **1** and **2**: both Fe1 and Fe2 in LS states at LS-LS phase; Fe1 in LS state and Fe2 in HS state at HS-LS phase; both Fe1 and Fe2 in HS states at HS-HS phase.

Table S1. Mössbauer hyperfine parameters of **2**.

1. Materials and General Procedures

All of the chemicals were obtained from commercial sources and used without further purification. The IR spectra were recorded from KBr disc in the range 4000-400 cm^{-1} with a Bruker-tensor 27 spectrometer.

2. PXRD Spectra

PXRD patterns of **1** and **2** were recorded on a D8 ADVANCE X-Ray Diffractometer (CuK α 0.154056 nm). The Rietveld refinement of the XRD pattern of **2** at 600 K was carried out using the program of Materials Studio.

3. X-Ray Crystallography

Diffraction intensities of **1** and **2** were collected on a Bruker SMART Apex CCD diffractometer with graphite-monochromated Mo K α radiation ($\lambda = 0.71073 \text{ \AA}$) or on a Rigaku R-AXIS SPIDER IP diffractometer (MoK α , $\lambda = 0.71073 \text{ \AA}$) at 293(2) and 383(2) K. The structures were solved by direct method, and all non-hydrogen atoms were refined anisotropically by least-squares on F^2 using the SHELXTL program. Hydrogen atoms on organic ligands were generated by the riding mode (G. M. Sheldrick, SHELXTL97, program for crystal structure refinement, University of Göttingen, Germany, 1997).

Crystal data for **1** at 293(2) K: $\text{C}_{24}\text{H}_{16}\text{FeN}_{10}$, 500.3 g mol^{-1} , triclinic, $P-1$, $a = 8.8471(12) \text{ \AA}$, $b = 9.1441(12) \text{ \AA}$, $c = 14.785(2) \text{ \AA}$, $\alpha = 94.125(2)^\circ$, $\beta = 103.444(2)^\circ$, $\gamma = 111.236(2)^\circ$, $V = 1068.1(2) \text{ \AA}^3$, $Z = 2$, $\rho = 1.556 \text{ g cm}^{-3}$. $R_1/wR_2 = 0.0386/0.0967$ ($I > 2\sigma(I)$).

Crystal data for **1** at 383(2) K: $a = 8.966(16) \text{ \AA}$, $b = 9.309(16) \text{ \AA}$, $c = 15.08(3) \text{ \AA}$, $\alpha = 94.38(3)^\circ$, $\beta = 102.90(4)^\circ$, $\gamma = 110.54(5)^\circ$, $V = 1132(4) \text{ \AA}^3$, $Z = 2$, $\rho = 1.467 \text{ g cm}^{-3}$. $R_1/wR_2 = 0.0372/0.0935$ ($I > 2\sigma(I)$).

Crystal data for **2** at 293(2) K: $\text{C}_{26}\text{H}_{20}\text{FeN}_{10}$, 528.4 g mol^{-1} , triclinic, $P-1$, $a = 9.3683(3) \text{ \AA}$, $b = 9.5284(4) \text{ \AA}$, $c = 14.3159(7) \text{ \AA}$, $\alpha = 93.456(1)^\circ$, $\beta = 104.500(1)^\circ$, $\gamma = 112.010(1)^\circ$, $V = 1130.00(8) \text{ \AA}^3$, $Z = 2$, $\rho = 1.553 \text{ g cm}^{-3}$. $R_1/wR_2 = 0.0374/0.0974$ ($I > 2\sigma(I)$).

Crystal data for **2** at 383(2) K: $a = 9.5062(9) \text{ \AA}$, $b = 9.6419(11) \text{ \AA}$, $c = 14.3420(19) \text{ \AA}$, $\alpha = 93.661(4)^\circ$, $\beta = 104.415(3)^\circ$, $\gamma = 111.004(3)^\circ$, $V = 1171.4(2) \text{ \AA}^3$, $Z = 2$, $\rho = 1.498 \text{ g cm}^{-3}$. $R_1/wR_2 = 0.0441/0.1233$ ($I > 2\sigma(I)$).

Unit cell parameters for **2** at 600 K from the refinement of PXRD data: $a = 9.561(4) \text{ \AA}$, $b = 9.786(4) \text{ \AA}$, $c = 14.624(6) \text{ \AA}$, $\alpha = 95.004(3)^\circ$, $\beta = 103.135(2)^\circ$, $\gamma = 112.135(2)^\circ$, $V = 1211.43 \text{ \AA}^3$. $R_{\text{wp}} = 2.81\%$, $R_p = 1.59\%$.

CCDC numbers: 824534 (**1**_293K), 824535 (**1**_383K), 824536 (**2**_293K), 824537 (**2**_383K) and 824538 (**2**_600K).

5. Magnetic measurements

Magnetic measurements were performed using a Quantum Design MPMS XL-7 SQUID magnetometer. The susceptibility measurements for **1** and **2** were first performed in the 2-380-2 K temperature range with an applied field of 2.0 kOe. Samples were sealed in parafilm to avoid any orientation of the crystallites. Then an oven was installed to take measurements from 380-600-380 K. Samples were wrapped in tinfoil. The magnetic data were corrected for the sample holder and diamagnetic contributions.

6. DSC measurements

DSC measurements were carried out on polycrystalline samples of **1** and **2** using a Netzsch DSC 204 F1 Phoenix instrument under nitrogen at a scan rate of 5 K min⁻¹ in both heating and cooling modes.

7. Mössbauer measurements

Mössbauer experiments were carried out by using a ⁵⁷Co/Rh source in a constant-acceleration transmission spectrometer. The spectrometer was calibrated by using a standard α -Fe foil.

8. Variable temperature Raman spectra measurements

Variable-temperature Raman spectra of **2** were collected using a Laser Micro-Raman Spectrometer (Renishaw inVia) with 514.5 nm laser source. Samples were enclosed in nitrogen atmosphere on the heat plate of a THMS600 (Linkam) liquid-nitrogen cryostage.

9. Simulation of the two-step SCO behaviors of **1** and **2**

Considering the large separation between the two sets of spin transition, inter-subset interaction was neglected here to simplify the simulation. Domain model^{1,2} was applied to simulate each SCO process (equations 1-6), and the two-step behavior was well reproduced by the sum of those two processes

$$\ln\left(\frac{1-\gamma_{HS1}}{\gamma_{HS1}}\right) = \frac{n_1\Delta H_1}{RT} - \frac{n_1\Delta S_1}{R} \quad (1)$$

$$\ln\left(\frac{1-\gamma_{HS2}}{\gamma_{HS2}}\right) = \frac{n_2\Delta H_2}{RT} - \frac{n_2\Delta S_2}{R} \quad (2)$$

$$\Delta H_1 = 2\Delta H_1(\text{exp}) \quad (3)$$

$$\Delta H_2 = 2\Delta H_2(\text{exp}) \quad (4)$$

$$\Delta S_1 = 2\Delta S_1(\text{exp}) = 2\Delta H_1/T_{c1} \quad (5)$$

$$\Delta S_2 = 2\Delta S_2(\text{exp}) = 2\Delta H_2/T_{c2} \quad (6)$$

where n stands for the number of molecules per domain; $\Delta H_{1,2}(\text{exp})$ and $\Delta S_{1,2}(\text{exp})$ are enthalpy and entropy variations deriving from DSC measurements; γ_{HS1} and γ_{HS2} are the spin fractions for each step and both taken to go from 0 to 1, and the total high spin fraction $\gamma_{HS} = (\gamma_{HS1} + \gamma_{HS2})/2$.

1. Sorai, M.; Seki, S. *J. Phys. Chem. Solids*, **1974**, *35*, 555.

2. Kahn, O. *Molecular Magnetism*, VCH, Weinheim, **1993**, pp. 67.

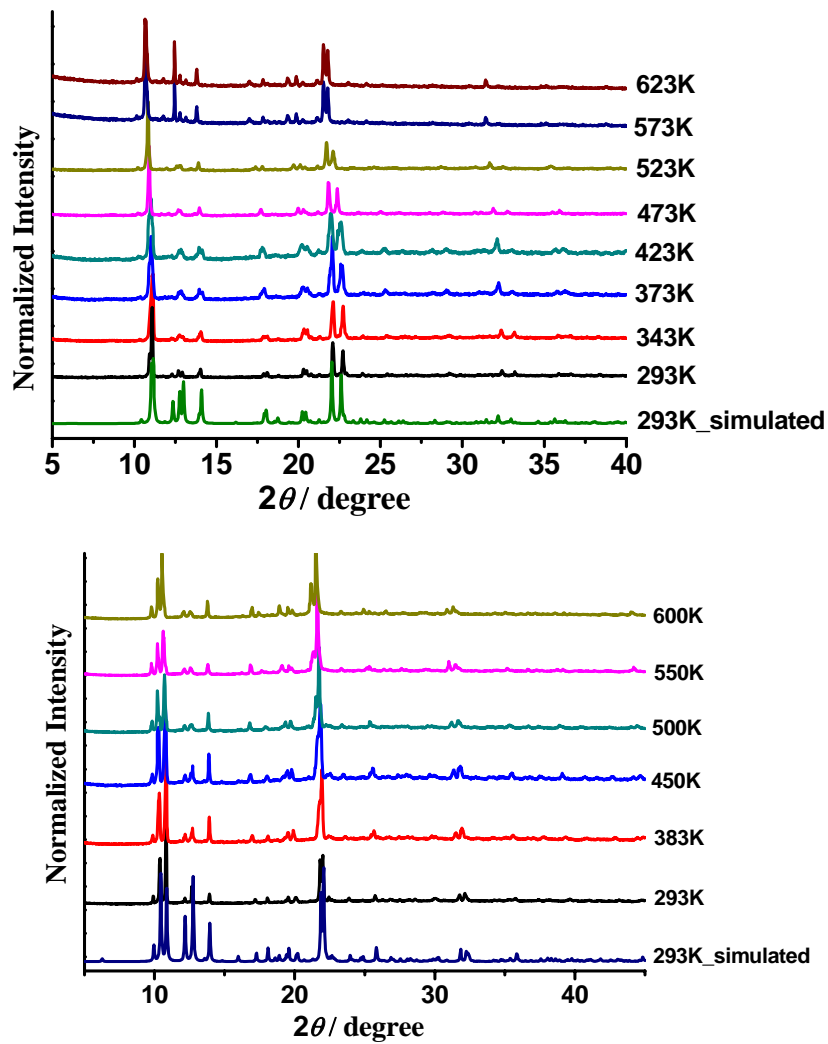


Fig. S1. Variable PXRD patterns for **1** (above) and **2** (below).

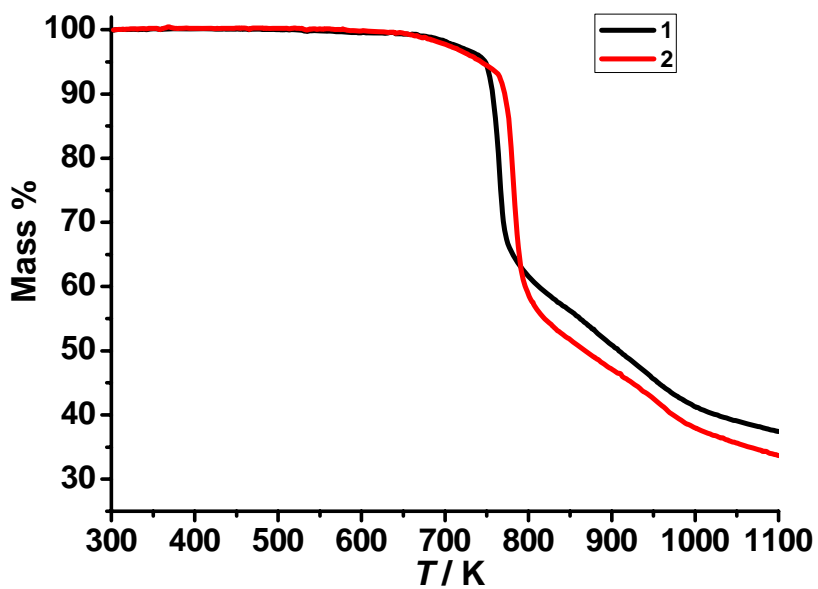


Fig. S2. TG curves for **1** (in black) and **2** (in red) under N₂ atmosphere.

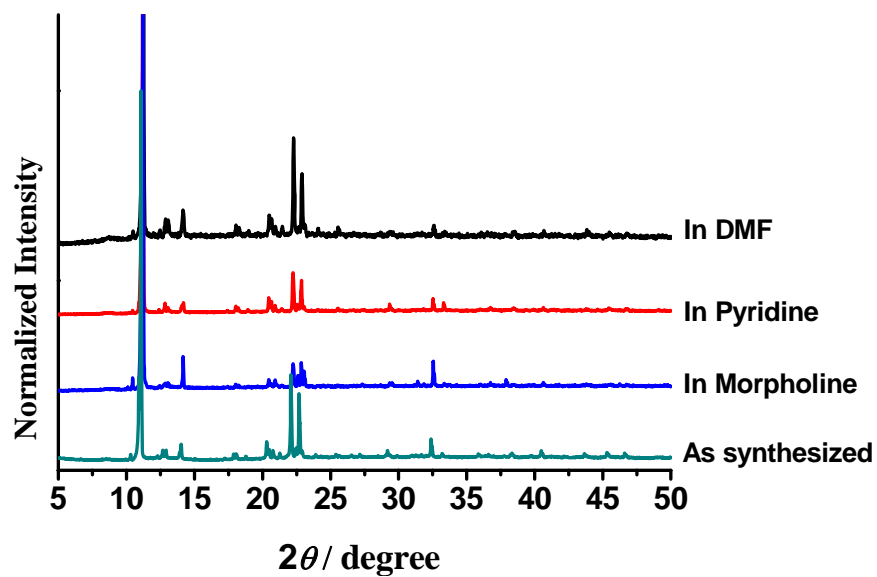


Fig. S3. PXRD patterns of **1** as-synthesized (in green) and of **1** immersing in morpholine (in blue), pyridine (in red) and DMF (in black) for one month.

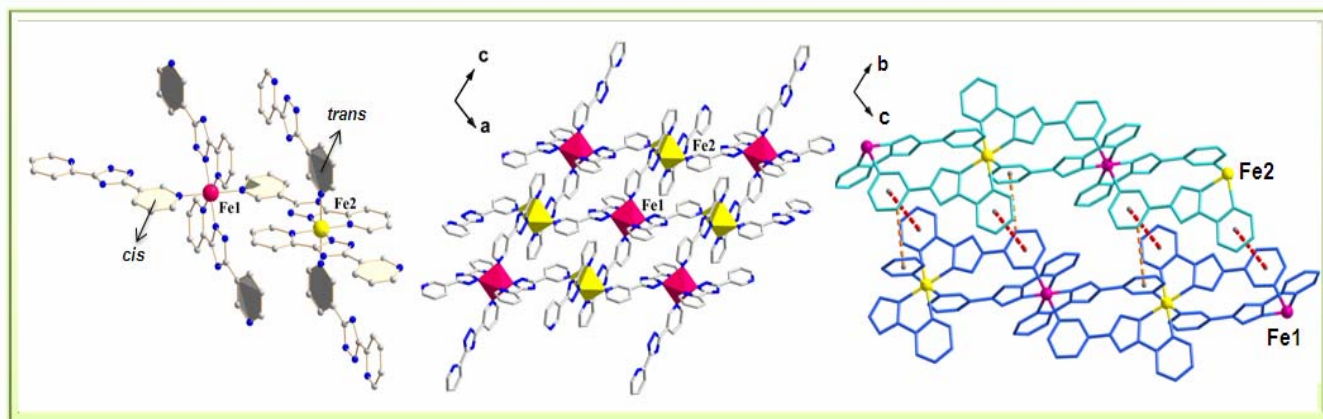


Fig. S4. Structural illustrations of **1**: Coordination environments of Fe1 and Fe2 (left); 2D (4,4) rhombic grids (middle); Crystal packing of two adjacent 2D layers highlighting the interlayer face-to-face $\pi \cdots \pi$ interactions (red dotted lines) and edge-to-face $\pi \cdots \pi$ interactions (orange dotted lines) (right). Hydrogen atoms have been omitted for clarity.

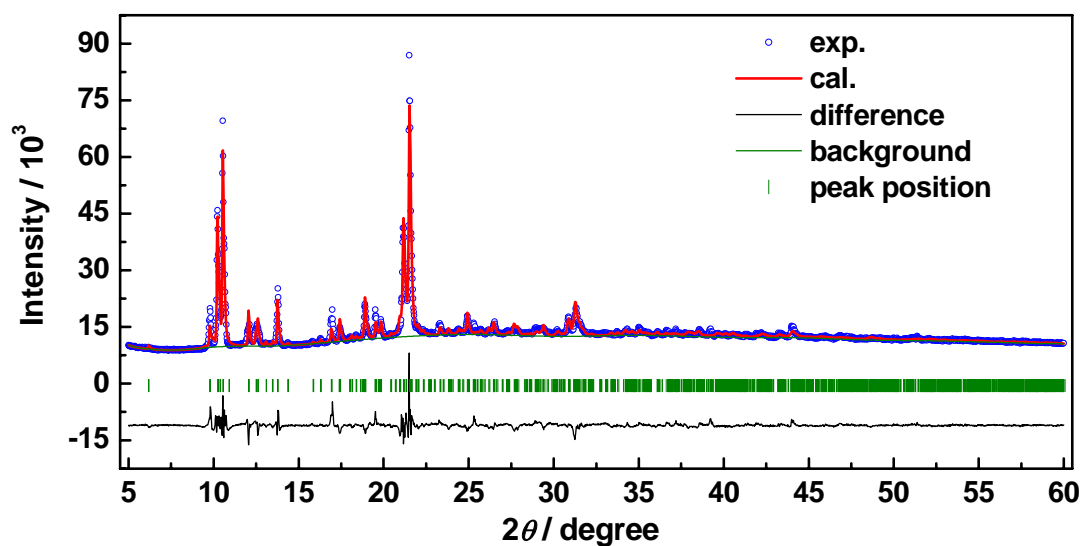


Fig. S5. Experimental PXRD (red continuous line) and Rietveld refined pattern (blue circles) and difference patterns (black line) for **2** at 600 K. The ticks are the position of the Bragg reflections, and the bottom trace is the residual. $R_{wp} = 4.35\%$, $R_p = 2.62\%$, $R_{comb} = 4.47\%$

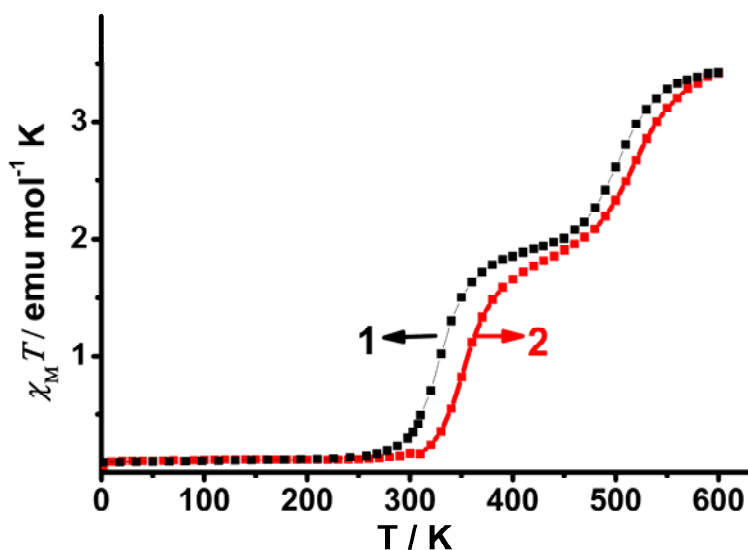


Fig. S6. The experimental $\chi_M T$ versus T curves of **1** and **2** in the temperature range 2-600 K.

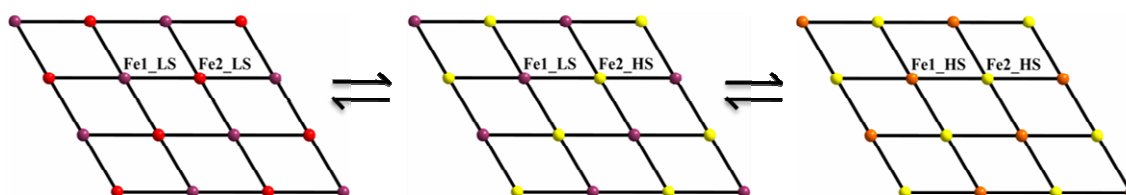


Fig. S8. Schematic of spin transition route for **1** and **2**: both Fe1 and Fe2 in LS states at LS-LS phase; Fe1 in LS state and Fe2 in HS state at HS-LS phase; both Fe1 and Fe2 in HS states at HS-HS phase.

Table 1. Mössbauer hyperfine parameters of the **2**, where δ is the isomer shift, ΔE_Q is the quadrupole splitting, Γ is the linewidth and RA is the relative spectral area of individual spectral components.

Temperature (K)	Component	$\delta \pm 0.01$ (mm/s)	$\Delta E_Q \pm 0.01$ (mm/s)	$\Gamma \pm 0.01$ (mm/s)	RA ± 1 (%)	Assignment
300	Doublet 1	0.41	0.77	0.27	50	LS Fe ²⁺
	Doublet 2	0.45	1.02	0.27	50	LS Fe ²⁺
375	Doublet 1	0.39	0.78	0.31	61	LS Fe ²⁺
	Doublet 2	0.71	1.11	0.31	39	HS Fe ²⁺
455	Doublet 1	0.40	0.69	0.31	57	LS Fe ²⁺
	Doublet 2	0.72	1.59	0.31	43	HS Fe ²⁺